PHYSICAL REVIEW A **82**, 063409 (2010)

Controlled dipole-dipole interactions between K Rydberg atoms in a laser-chopped effusive beam

M. R. Kutteruf and R. R. Jones[*]
Department of Physics, University of Virginia, Charlottesville, Virginia 22904-4714, USA

(Received 20 October 2010; published 16 December 2010)

We explore pulsed-field control of resonant dipole-dipole interactions between K Rydberg atoms. A laser-based atomic beam chopper is used to reduce the relative velocities of Rydberg atoms excited from an effusive thermal source. Resonant energy transfer (RET) between pairs of atoms is controlled via Stark tuning of the relevant Rydberg energy levels. Resonance line shapes in the electric field dependence of the RET probability are used to determine the effective temperature of the sample. We demonstrate that the relative atom velocities can be reduced to the point where the duration of the electric-field tuning pulses, and not the motion of neighboring atoms, defines the interaction time for each pair within the ensemble. Coherent, transform-limited broadening of the resonance line shape is observed as the tuning pulse duration is reduced below the natural time scale for collisions.

DOI: 10.1103/PhysRevA.82.063409 PACS number(s): 32.80.Ee, 37.20.+j

I. INTRODUCTION

Dipole-dipole (DD) interactions between neutral atoms or molecules underlie a variety of fundamental few- and many-body physics problems. Those involving Rydberg atoms can be substantial, even at long range, and are interesting for exploring diverse phenomena, from quantum information processing [1–3] to the spontaneous evolution of Rydberg gases, to cold neutral plasmas [4–6]. Controlled resonant energy transfer (RET) between Rydberg atoms has proven to be a convenient method to explore DD interactions [7–23]. The simplest form of RET occurs between atom pairs when an electron on one atom, A, donates energy to an electron on atom B. In a perfectly resonant process, no energy is transferred to additional degrees of freedom and the electronic energy of the pair is conserved [24]. Such Förster resonances [25] are rare for pairs of atoms in low-lying levels, but they are more common in Rydberg systems because of the high density of available electronic states. Moreover, owing to the large polarizabilities of Rydberg atoms, resonant interactions can be induced via Stark tuning of Rydberg energy levels through the application of small electric fields.

Measurements of RET between Rydberg atoms have been made in room-temperature vapor cells, atomic beams, and in magneto-optical traps (MOTs) [7–15,24,26]. In a MOT, Rydberg atoms are nearly frozen over the microsecond time scales required for RET, and the resonant atom-atom coupling is conveniently described in terms of (nearly) static DD interactions of the form $V_{\mathrm{DD}} \sim \frac{\mu_A \mu_B}{R^3}$ (a.u.), where μ_A and μ_B are the dipole moments of two atoms, A and B, separated by a distance R. The values of μ_A and μ_B depend on the specific Rydberg levels of interest, but can have magnitudes on the order of n^2 for transitions between states with the same principal quantum number, n [24]. Thus, typical RET rates within an ensemble can approach $\Gamma = \frac{\mu_A \mu_B}{\langle R \rangle^3} \sim 2\pi\rho n^4$ (a.u.), or >1 MHz for $n > 20$ and $\rho > 10^9$ cm^{-3}. For temperatures $T \sim 100$ μK and densities $\rho \sim 10^9$ cm^{-3}, typical atoms in a MOT move only a few percent of the average interatomic separation $\langle R \rangle \approx (2\pi\rho)^{-1/3} \approx 5$ μm during the $\sim$1 μs time interval required to transfer substantial population via RET. In this case, pulsed electric fields can be used as controls to tune atom pairs into and out of resonance, turning on and off the DD coupling, at well-defined times [14]. Even if the separation between atoms is not precisely known or uniform throughout the sample, the ability to affect RET at specific times enables a variety of time-domain spectroscopies that can be used to characterize interactions between Rydberg atoms in an ensemble. For example, time-domain Ramsey interferometry for probing dephasing [14] and echo methods for quantifying coherence both rely on pulsed interactions during well-defined intervals [27].

It is not currently possible to laser cool and/or trap all atomic and molecular species that might exhibit interesting dynamics in this context. Even so, in principle, time-domain studies of RET can be performed in any Rydberg sample, provided the DD coupling can be pulsed on and off in a sufficiently short time interval, τ, during which typical atoms experience little variation in V_{DD}. Therefore, it is prudent to estimate the values of τ required to make such measurements. Consider a three-dimensional gas of Rydberg atoms of mass M. The rms relative velocity between atoms is $v_{\mathrm{rms}} = \sqrt{6kT/M}$, where k is Boltzmann's constant. The DD coupling between atoms will be approximately constant during a time interval τ if the distance traveled during that interval is much less than the nearest-neighbor separation between typical atoms in the ensemble $v_{\mathrm{rms}}\tau \ll (2\pi\rho)^{-1/3}$. Assuming a near maximum dipole moment for a given n state, $\mu_1 \sim \mu_2 \sim n^2$, the RET amplitude during the interval τ is $\eta = \Gamma\tau \sim 2\pi\rho n^4 \tau$ (a.u.). By using this expression to eliminate ρ from the preceding inequality, we obtain $\tau \ll \frac{n^2}{\sqrt{\eta v_{\mathrm{rms}}^3}}$ (a.u.) as a requirement to ensure roughly constant V_{DD} during the interval τ.

At $T = 300$ K, $v_{\mathrm{rms}} > 400$ m/s for typical atoms and small molecules, such that $\tau \ll 30n^2$ ps even for a transition probability as small as $\eta^2 = 1\%$. Accordingly, effective switching of RET for Rydberg atoms with $n = 20$ requires the application of constant-amplitude electric-field pulses with durations $\tau \ll 10$ ns and Rydberg densities $\rho \gg 10^9$ cm^{-3}. Generating the constant amplitude, $\tau \sim 1$ ns field pulses needed to define single Rydberg interaction times would be a significant technical challenge for experiments. Performing time-domain spectroscopies with multiple, precisely delayed interactions

---

[*] bjones@virginia.edu

within the requisite ∼1 ns time window would be extremely difficult, if not impossible [27]. Moreover, at such high Rydberg densities, nonresonant van der Waals interactions play a non-negligible role, complicating the dynamics [28–30]. Working at significantly higher n affords the use of longer pulses and lower densities, but also makes the experiments much more sensitive to the deleterious effects of stray fields, field inhomogeneities, and increased van der Waals interactions.

At lower temperatures, not necessarily as low as those reached in a MOT, the experimental constraints relax considerably. For $T = 10$ K, the relative atom or molecule speeds are reduced to $v_{\text{rms}} \sim 70$ m/s and DD interactions between atom pairs remain constant for times $\tau \ll n^2$ ns for $\eta \sim 1\%$. Accordingly, it should be possible to perform time-domain experiments by using electric-field pulses and pulse sequences with durations of ∼100 ns to toggle DD interactions between $n \sim 20$ atoms. With longer interaction times the RET rate can be reduced while maintaining comparable yields. Thus, at lower temperatures experiments can be conducted at reduced densities, $\rho < 10^8$ cm^{-3}, where the effects of nonresonant interactions are small.

Several previous experiments on coherent DD interactions between atoms have utilized mechanical methods to reduce the relative velocities of atoms in atomic beams. For example, Stoneman, Adams, and Gallagher used thermal expansion of a mechanically chopped atomic beam to effectively cool K atoms [26]. In their method, a spinning disk produces spatially localized atom pulses of length d. Each atom pulse expands longitudinally while traveling for a time Δt prior to laser excitation to Rydberg states. The longitudinal spreading reduces the relative atom velocities, Δv, by a factor $\sqrt{\kappa} \propto d/\Delta t$ [26]. Application of electric-field pulses with durations of $\tau \sim 500$ ns then allowed Thomson, Renn, and Gallagher to gate the DD interaction to control RET between the atoms [8]. The same technique enabled Renn *et al.* to explore radiatively assisted RET [9,31]. By phase locking the DD interactions with a microwave driving field, they confirmed atom pair coherence over multiple interaction times. More recently, Saquet *et al.* used a supersonic expansion to produce a fast sodium beam with an effective temperature of ∼1 K [23]. The small relative atom velocities allowed them to control RET between atom pairs by using pulsed electric-field ramps to sweep atoms through resonance, driving adiabatic Landau-Zener transitions between pair states coupled by the DD interaction.

Here we present measurements demonstrating temporally controlled RET between K Rydberg atoms in a thermal beam. The results are similar to those of Thomson, Renn, and Gallagher [8], but are obtained without the use of a mechanical chopper. Specifically, we examine the $29s_{1/2} + 27d_{3/2} \rightarrow 29p_{1/2} + 28p_{1/2}$ RET process in potassium, which occurs in an externally applied electric field $F_0 \approx 6.43$ V/cm [26]. Velocity reduction is achieved by focusing Rydberg excitation lasers of diameter d across the thermal beam and waiting a time Δt before applying an electric-field pulse that Stark tunes the Rydberg atoms in and out of DD resonance. In analogy with the mechanical chopper, the laser creates a pulse of Rydberg atoms within the atomic beam. The pulse spreads longitudinally owing to the thermal velocity distribution of the atoms, decreasing the relative velocity, Δv, of neighboring Rydberg atoms by a factor $\sqrt{\kappa}$.

An obvious advantage of the laser-chopper technique presented here is that it eliminates the spinning chopper wheel and its high-speed motor, along with the mechanical alignment, timing, and vacuum problems they present. Also, because d is determined by the diameter of a focused laser, atom pulses with lengths that are orders of magnitude smaller than those attainable from mechanically chopped beams can be produced. Accordingly, expansion times, Δt, that are orders of magnitude smaller give the same relative velocity reduction. Therefore, because the final atom density is inversely proportional to Δt, a substantially lower atomic beam flux can be used to obtain the same atom density in the velocity-reduced sample.

In the following sections first we describe the experimental apparatus and approach. Next, the results of the experiments, demonstrating both effective cooling of the atomic beam and coherent broadening of RET resonances owing to temporal gating of RET, are presented. We then derive expressions for the atom density and relative velocity distribution as a function of expansion time in the laser-chopped beam. We present a two-atom model for RET that allows us to calculate the width and maximum transition probability of the electric-field-tuned RET resonance. Estimates for the reduced beam temperature and density are then extracted from the measured RET line shapes and compared to model predictions. We conclude by summarizing our results and discussing potential applications of the laser-chopper technique.

II. EXPERIMENTAL APPARATUS AND APPROACH

The experiments are performed at a 15-Hz repetition rate in a vacuum chamber with a background pressure of $\sim 10^{-6}$ Torr. Three 5-ns pulsed dye lasers excite atoms from a thermal K beam into $29s_{1/2}$ and $27d_{3/2}$ Rydberg states, as shown in Fig. 1. The first laser drives the $4s \rightarrow 4p_{1/2}$ transition at 770.1 nm. The other two lasers are tuned to ∼457 nm and transfer population from the $4p_{1/2}$ state to the two Rydberg states. The parallel laser beams are focused with a single 350-mm lens and cross the K beam at right angles. The overlapping beams have full width at half maximum (FWHM) diameters of $d \sim 130$ μm, exciting a cylinder of atoms between two parallel aluminum field plates. The field plates are square, 7.5 cm on a side, and are separated by 0.64 cm. Static and/or pulsed voltages applied to the electric-field plates create a uniform electric field, enabling Stark tuning of the DD interactions. The three lasers pulses are polarized parallel to the applied electric field, are temporally overlapped when they cross the K beam, and have sufficient flux to saturate their respective transitions. Therefore, one-quarter of the atoms that are exposed to the laser beams are excited to each of the two Rydberg states.

The laser excitation proceeds in a static electric field, F_s, created by applying a constant voltage to the lower field plate. Typically, the static excitation field is set to a value that is too large for RET $29s_{1/2} + 27d_{3/2} \rightarrow 28p_{1/2} + 29p_{1/2}$ to occur between pairs of atoms (see Fig. 1). Instead, the volume of noninteracting Rydberg atoms is allowed to expand for a time Δt beneath a 0.2 cm × 2.5 cm slit in the upper field plate.

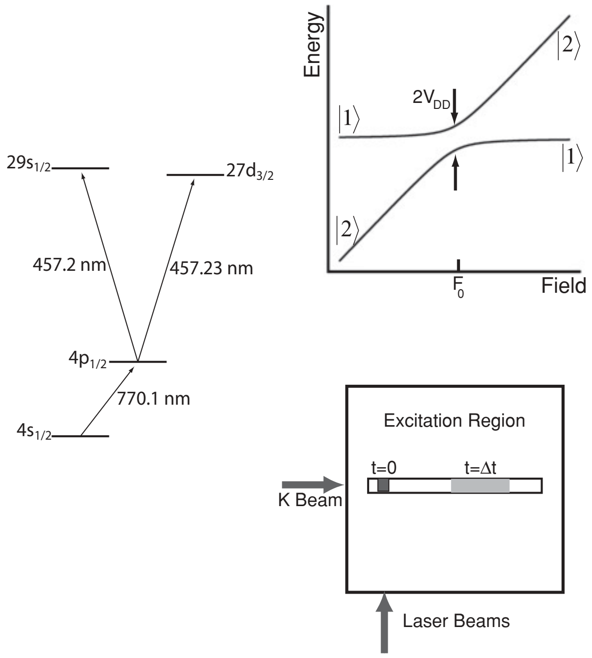

FIG. 1. (Left) Schematic of the laser excitation scheme used to create the $29s_{1/2}$ and $27d_{3/2}$ Rydberg atoms. (Upper right) Schematic of the interacting pair states as a function of electric field in a two-state approximation. At large R, or fields $F \neq F_0$, the eigenstates are $|1\rangle = |29s_{1/2}\rangle|27d_{3/2}\rangle$ and $|2\rangle = |28p_{1/2}\rangle|29p_{1/2}\rangle$. RET occurs in the avoided level crossing region at electric fields $F \sim F_0 = 6.43$ V/cm, where the eigenstates are linear combinations of $|1\rangle$ and $|2\rangle$. The energy gap at the avoided crossing is $2V_{\mathrm{DD}}$, which varies with the relative separation between atoms in a pair. (Lower right) Schematic of the laser excitation and atom expansion region beneath the slit in the upper electric-field plates. The small dark gray region near the left edge of the slit shows the initial atom excitation region. The larger, light gray region near the center of the slit depicts the excited atoms after they have expanded for a time Δt.

The DD interaction is then toggled on and off by applying a 2-V pulse to the upper field plate, reducing the electric field to $F \sim F_0$. The tuning pulse is produced by an arbitrary waveform generator and has a duration τ with a <2 ns rise time. The pulse projects the Rydberg atoms from the high-field, noninteracting states to a coupled basis of interacting levels near F_0 (see Fig. 1). Thus, τ defines the maximum time during which RET can occur.

Immediately after the tuning pulse, the total Rydberg signal and the fraction of atoms undergoing resonant energy transfer are measured via state-selective field ionization (SSFI). A high-voltage ramp is applied to the lower field plate, ionizing any Rydberg atoms in the interaction region, and pushing the resulting ions through the slit in the upper field plate toward a microchannel plate detector. It is worth noting that following excitation, the Rydberg ensemble expands longitudinally along the slit, but experiences negligible transverse spreading prior to the field ionization ramp. Thus, any Rydberg atoms that are excited beneath the slit remain beneath the slit and can be detected via SSFI. Half of the atoms undergoing RET are excited to the $29p_{1/2}$ level, so the ratio of the $29p_{1/2}$ to total Rydberg atoms detected gives the RET probability per atom pair, P.

We measure P as a function of the net electric field, F, by varying F_s on successive laser shots. The independent axis for these resonance line shapes is then converted from F to energy detuning, E, by using the known field dependence of the energy splitting between noninteracting $|29s_{1/2}\rangle|27d_{3/2}\rangle$ and $|28p_{1/2}\rangle|29p_{1/2}\rangle$ atom pairs. The detuning varies quadratically with electric field, with a slope of 2.46 MHz/(V/cm)^2 [26]. The variations in the resonance line shapes as functions of Δt and τ are used to characterize the relative velocity reduction in the thermal expansion, as well as confirm the coherence of the DD interaction over short time scales.

III. EXPERIMENTAL RESULTS

Figure 2 shows the measured resonance line shapes for several different expansion times, Δt, at a fixed tuning pulse duration, $\tau = 1$ μs. These data are collected in the "long-pulse" regime in which the duration of DD interactions is limited by the relative motion of atoms rather than the tuning pulse. In other words, as described in detail in Sec. IV, $\tau > \tau_0$, where $\tau_0 = 2b_0/v_0$ is a typical collision time, v_0 is the average relative speed between Rydberg atoms, and b_0 is the distance of closest approach between the Rydberg atoms that contribute most to the RET signal. Inspection of the line-shape data shows that under long-pulse conditions, both the maximum RET probability, P_0, and the resonance width, ΔE, decrease as Δt is increased. Qualitatively, this is expected from the thermal expansion. First, because the RET probability is proportional to ρ, P_0 decreases as Δt increases. Second, as described in detail in Sec. IV, v_0 shrinks as the ensemble expands. The growth in b_0 and decrease in v_0 result in an

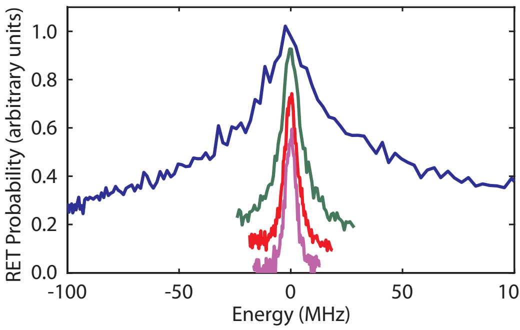

FIG. 2. (Color online) RET probability, P, vs energy detuning, E, for several different expansion times, Δt. Ordered from top to bottom, the blue, green, red, and violet curves correspond to $\Delta t = 0$, 0.5, 1.0, and 1.5 μs, respectively. For clarity, the curves have been vertically offset from each other and the amplitudes of the green, red, and violet line shapes have been multiplied by factors of 3, 4, and 6, respectively. All data were collected in the "long-pulse" regime, $\tau > \tau_0$, where the motion of atoms, not the detuning pulse, determines the duration of the interaction between atoms. The green, red, and violet curves were collected with a tuning pulse duration, $\tau = 1$ μs. The blue (upper) curve was measured without a tuning pulse because, for this broad resonance, the 3.1 V/cm tuning pulse amplitude was insufficient to tune the atoms from far off resonance to on resonance. In this case the atoms are allowed to interact for the full 2-μs interval between the laser excitation and field ionization, but the width and peak amplitude of the resonance are independent of the interaction time for $\tau > 1$ μs.

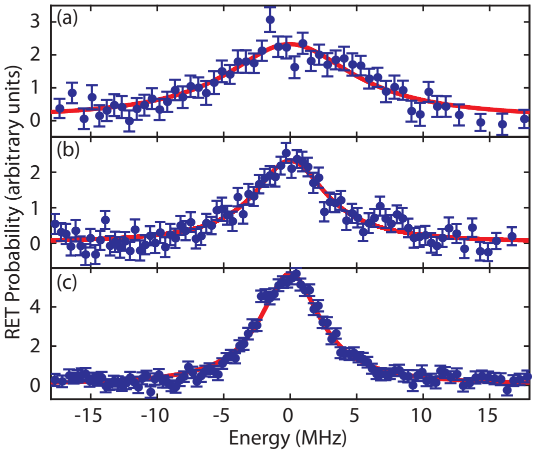

FIG. 3. (Color online) RET probability, P, vs energy detuning, E, for several different tuning pulse durations for a fixed expansion time, $\Delta t = 1.5\ \mu$s. The line shapes exhibit coherent Fourier-transform broadening as the tuning pulse duration is reduced below the typical interaction time between moving atoms, $\tau_0 \sim 500$ ns. In (c), $\tau = 1\ \mu$s and the resonance width $\Delta E = 5.5 \pm 0.2$ MHz. In (b), $\tau = 200$ ns and $\Delta E = 6.7 \pm 0.6$ MHz. In (a), $\tau = 100$ ns and $\Delta E = 11.8 \pm 1.2$ MHz. For all three graphs the dots are measurements with associated uncertainties and the solid lines are Lorentzian fits to those data.

increase in the interaction time τ_0 and, in accordance with the uncertainty principle, a concomitant reduction in ΔE.

Figure 3 shows the measured line shapes as τ is reduced below $\tau_0 \simeq 500$ ns for a fixed expansion time, $\Delta t = 1.5\ \mu$s. For $\tau > \tau_0$, the resonance widths are determined by the Rydberg density and relative velocity distribution, and are independent of τ. However, for $\tau < \tau_0$, the interaction time between typical atoms is restricted by the tuning pulse. In this "short-pulse" regime, the resonance linewidth is determined solely by the tuning pulse duration that is under our control. Figure 3 shows that, in agreement with our expectations from the uncertainty principle, in the short-pulse regime the resonance widths increase as τ decreases. This "transform-limited" broadening reflects the coherence of the Rydberg-Rydberg dynamics within the ensemble. The substantial increase in ΔE observed for $\tau = 100$ ns indicates that essentially all interactions within the ensemble begin and end at the same times. This coherent control over the Rydberg-Rydberg coupling is made possible by the effective cooling of the relative atom motion in the thermal expansion.

IV. ANALYSIS

To obtain a quantitative understanding of the results presented in Figs. 2 and 3, first we derive expressions for the Rydberg density and the relative velocity distribution of neighboring Rydberg atoms as a function of the expansion time, Δt. We then present a two-atom model that approximates the Rydberg-Rydberg interactions within the beam. Comparisons between simulation results based on this model and the data shown in Fig. 2 are used to extract the Rydberg atom density and effective temperature as a function of Δt. These density and temperature determinations are then used to simulate the transform broadening of the RET line shapes as a function of tuning pulse duration data. The predicted resonance widths are found to be in good agreement with measurements such as those shown in Fig. 3.

A. Delay dependence of the Rydberg density

Consider a collimated atomic beam propagating in the $+z$ direction that is crossed by a Gaussian laser beam(s) propagating in the $+x$ direction. At a time $t = 0$, the laser excitation defines the spatial probability distribution for finding a Rydberg atom at a location, z_0, along the atomic beam, relative to the axis of the laser beam,

$$D(z_0) = \frac{1}{\sqrt{\pi}d} \exp\left(-z_0^2/d^2\right), \tag{1}$$

where the pulse width d is related to the FWHM of the laser beam, $d_0 = 2\sqrt{\ln(2)}d$. At this time, the velocity distribution of Rydberg atoms within the excitation volume is equal to that of the beam [32],

$$f(v) = \frac{1}{2}\left(\frac{M}{kT}\right)^2 v^3 \exp\left(-\frac{M}{2kT}v^2\right). \tag{2}$$

At a time $t = \Delta t$ after the laser excitation, the probability distribution is

$$D(z) = \int_0^\infty f(v) D(z - v\Delta t)\, dv, \tag{3}$$

where $z = z_0 + v\Delta t$ is the Rydberg atom's position along the beam propagation direction after a delay Δt. The integral in Eq. (3) cannot be expressed in closed form. However, by first considering the relative position and relative velocity distributions of Rydberg atoms in the pulse, we can obtain a simple expression that is an excellent approximation to the exact probability distribution of Eq. (3).

First, we note that the distribution of relative Rydberg atom positions along the beam $D(\Delta z)$ can be obtained by integrating over the probabilities for finding atom 1 with velocity v_1 at position $z_1 = z_1' + v_1\Delta t$ and atom 2 with velocity v_2 at position $z_2 = z_2' + v_2\Delta t$, such that $\Delta z = z_2 - z_1$:

$$\begin{aligned} D(\Delta z) = &\int_0^\infty dv_1 \int_0^\infty dv_2 \int_{-\infty}^\infty dz_1 f(v_1) D(z_1 - v_1\Delta t) \\ &\times f(v_2) D(z_1 + \Delta z - v_2\Delta t). \end{aligned} \tag{4}$$

Because the two spatial distribution functions are Gaussian, the integral over z_1 is done easily, resulting in

$$\begin{aligned} D(\Delta z) = &\frac{1}{\sqrt{2\pi}d} \int_0^\infty dv_1 \int_0^\infty dv_2 f(v_1) f(v_2) \\ &\times \exp\left[-\frac{(v_2\Delta t - v_1\Delta t - \Delta z)^2}{2d^2}\right]. \end{aligned} \tag{5}$$

By writing $v_2 = v_1 + \Delta v$, where Δv is the relative velocity of the two atoms, one obtains

$$\begin{aligned} D(\Delta z) = &\frac{1}{\sqrt{2\pi}d} \int_0^\infty dv_1 \int_{-\infty}^\infty f(v_1) f(\Delta v + v_1) \\ &\times \exp\left[-\frac{(\Delta v\Delta t - \Delta z)^2}{2d^2}\right] d\Delta v. \end{aligned} \tag{6}$$

Now, one of the integrals in Eq. (6),

$$f(\Delta v) = \int_0^\infty f(v_1) f(\Delta v + v_1)\, dv_1, \tag{7}$$

is the relative velocity distribution for atom pairs in the beam. It cannot be written in closed form. However,

$$f(\Delta v) \simeq \sqrt{\frac{M}{2\pi k T'}} \exp\left(-\frac{M\Delta v^2}{2kT'}\right) \tag{8}$$

is an excellent approximation. For $T' \simeq T/1.07682$, the difference between the approximate and the exact form for $f(\Delta v)$ is less than 1% for values of Δv for which $f(\Delta v)$ is greater than 10% of its maximum. In addition, the values for the average relative speed v_0 and rms relative velocity obtained from the approximate expression are within 0.1% of their correct values. Substituting this approximation for $f(\Delta v)$ in Eq. (6), we obtain

$$D(\Delta z) = \frac{1}{2\pi d}\sqrt{\frac{M}{kT'}} \int_{-\infty}^{\infty} \exp\left(-\frac{M\Delta v^2}{2kT'}\right) \times \exp\left[-\frac{(\Delta v \Delta t - \Delta z)^2}{2d^2}\right] d\Delta v. \tag{9}$$

The remaining integral is easily performed, yielding

$$D(\Delta z) \simeq \frac{1}{\sqrt{2\pi\kappa d^2}} \exp\left(-\frac{\Delta z^2}{2\kappa d^2}\right), \tag{10}$$

where

$$\kappa = 1 + \frac{\Delta t^2 k T'}{M d^2} \tag{11}$$

is a delay-dependent expansion factor. In terms of the average velocity $\bar{v} = \sqrt{\frac{9\pi kT}{8M}}$ in the atomic beam, $\kappa \simeq 1 + (\frac{\bar{v}\Delta t}{2d})^2$.

The relative position distribution $D(\Delta z)$ is the autocorrelation function of the position distribution function that we seek, $D(z)$. Because $D(\Delta z)$ is Gaussian, and the autocorrelation function of a Gaussian is another Gaussian with a FWHM that is $\sqrt{2}$ times greater than the original, an excellent approximation for $D(z)$ (in a reference frame moving with the center of the Rydberg pulse) is

$$D(z) \simeq \frac{1}{\sqrt{\pi\kappa d^2}} \exp\left(-\frac{z^2}{\kappa d^2}\right). \tag{12}$$

This expression has precisely the same form as that for the initial Rydberg distribution function [Eq. (1)] except that the Rydberg pulse width has increased from d to $\sqrt{\kappa}d$ after a delay Δt. Therefore, assuming negligible expansion of the beam in the transverse dimensions, the Rydberg density decreases with increasing delay as $\rho = \rho_0/\sqrt{\kappa}$, where ρ_0 is the Rydberg atom density immediately following the laser excitation. Note that $\kappa \gg 1$ when the expansion time $\Delta t \gg d/\bar{v}$, where $d/\bar{v}$ is the time the average atom requires to traverse the excitation region. In this large expansion limit, $\sqrt{\kappa} \simeq \frac{\bar{v}\Delta t}{2d}$, and the density decreases in inverse proportion to Δt.

B. Delay dependence of the relative velocity of interacting Rydberg atoms

Next we consider the relative velocity distribution for neighboring atoms as a function of Δt. From the integrand of Eq. (9) we define the probability density,

$$P(\Delta z, \Delta v) = \frac{1}{2\pi d}\sqrt{\frac{M}{kT'}} \exp\left(-\frac{M\Delta v^2}{2kT'}\right) \times \exp\left[-\frac{(\Delta v \Delta t - \Delta z)^2}{2d^2}\right], \tag{13}$$

such that $f(\Delta v) = \int_{-\infty}^{\infty} P(\Delta z, \Delta v)\, d\Delta z$ is the relative velocity distribution of all the Rydberg atoms in the pulse as a function of delay. However, when considering atom-atom interactions, our interest is not in the full relative velocity distribution, but rather the relative velocity distribution,

$$f_0(\Delta v) = \int_{-\delta}^{\delta} P(\Delta z, \Delta v)\, d\Delta z, \tag{14}$$

of neighboring atoms for which $|\Delta z| \leqslant \delta$. Here δ is the typical distance over which Rydberg-Rydberg interactions are non-negligible. Because the microscopic distance δ is much smaller than $\Delta v \Delta t$ for nearly all the atoms in our sample, at the delays of interest in our experiments, we can approximate $f_0(\Delta v)$ by setting $\Delta z = 0$ in the integrand of Eq. (14). This yields

$$f_0(\Delta v) \simeq \frac{\delta}{\pi d}\sqrt{\frac{M}{2\pi kT'}} \exp\left(-\frac{M\kappa\Delta v^2}{2kT'}\right), \tag{15}$$

which has the same form as the relative velocity distribution in the original beam, but with an effective temperature, T'/κ, which decreases as the Rydberg pulse expands. In particular, in the long expansion limit for which $\kappa \gg 1$, the effective temperature drops in inverse proportion to the square of the expansion time, Δt. This effective cooling can be quite significant even for relatively short expansion times. For example, for potassium Rydberg atoms excited in a 500-K thermal beam by using a laser with a FWHM diameter $d_0 = 100\ \mu$m, $\kappa \simeq 125$, and $T_0 = 4$ K for $\Delta t = 2\ \mu$s.

C. Two-atom DD model

Next we develop a model for the predominant DD interactions between pairs of atoms. This model enables us to compute the RET resonance widths and peak transition probabilities for a given Rydberg atom density and relative velocity distribution. Neglecting interactions beyond nearest neighbors, the Hamiltonian for a pair of Rydberg atoms is

$$H = H_A + H_B + V, \tag{16}$$

where H_A and H_B are the Hamiltonians for individual atoms A and B in a static electric field, and V is the interaction potential between atoms. By assuming the distance between the atoms, R, is much greater than the radial extent of the Rydberg electron on either atom, V can be approximated by a pure dipole-dipole interaction [33]:

$$V_{\mathrm{DD}} = [\vec{r}_A \cdot \vec{r}_B - 3(\vec{r}_A \cdot \hat{R})(\vec{r}_B \cdot \hat{R})]/R^3, \tag{17}$$

where $\vec{r_A}$ and $\vec{r_B}$ are the Rydberg electron positions on atoms A and B relative to their respective nuclei, $\vec{R}$ is the location of the nucleus of atom B relative to that of atom A, and (unless otherwise noted) atomic units are assumed. Defining $\hat{z} = \hat{R}$, Eq. (17) simplifies to

$$V_{\mathrm{DD}} = r_A r_B \left(C_{1,1}^{(A)} C_{1,-1}^{(B)} + C_{1,-1}^{(A)} C_{1,1}^{(B)} - 2C_{1,0}^{(A)} C_{1,0}^{(B)}\right) / R^3, \quad (18)$$

where $C_{k,q}^{(j)}$ is a spherical tensor operator acting on atom j. The $C_{k,q}$ are proportional to spherical harmonics $C_{k,q} = \sqrt{\frac{4\pi}{2k+1}} Y_{k,q}$.

Ignoring spin, a single initial atom pair $\psi_0 = |29s, m_A = 0\rangle|27d, m_B\rangle$ is coupled to several degenerate final states, $\psi_i = |29p, m'_A\rangle|28p, m'_B\rangle$ or $|28p, m'_A\rangle|29p, m'_B\rangle$, with one, two, or three different combinations of m'_A and m'_B for $|m_B| = 2$, 1, or 0, respectively. We can diagonalize the Hamiltonian, H, in this basis of essential states for each m_B. The diagonalization reveals an effective two-level system with ψ_0 coupled to a single final state, ψ', that is constructed from a linear combination of the ψ_i. The two interacting levels exhibit an electric-field dependence that is identical to that shown schematically in Fig. 1, with an m_B-dependent scalar coupling $V_{\mathrm{DD}}(m_B) = \sqrt{\sum_i |\langle\psi_0|V_{\mathrm{DD}}|\psi_i\rangle|^2}$. Lastly, because all possible orientations of atom B relative to the internuclear direction $\hat{R}$ are possible, we define an angle-averaged interaction strength, $V_{\mathrm{DD}} = \sum_{m_B} V_{\mathrm{DD}}(m_B)/5$, which has the form $\mu_A\mu_B/R^3$. The most probable value of V_{DD} for a typical atom pair in a random ensemble at density ρ is $V_0 \simeq 3\pi\mu_A\mu_B\rho$. By using a Numerov integration to compute the radial matrix elements and standard angular momentum algebra, we find the product of the effective dipole matrix elements $\mu_A\mu_B \simeq 4.9 \times 10^5$ (a.u.). It is worth noting that the interacting states have an average effective principal quantum number, $\bar{n} = 26.8$, so $\mu_A\mu_B \simeq 0.95\bar{n}^4$ is nearly equal to its maximum value.

D. Resonance width in the long- and short-pulse regimes

In the experiments, the time interval $\mathcal{T}$ during which two atoms interact is limited either by the relative motion of the atoms or by the duration τ of the tuning field pulse. To simulate the effects of the relative velocity reduction and the temporal gating of the interactions (see Figs. 2 and 3), we use a pulsed, constant-interaction model to approximate the $\mathcal{T}$ dependence of the measured resonance line shapes.

Following the laser excitation, atoms in the $|29s\rangle$ and $|27d\rangle$ states are detuned very far from resonance and are effectively noninteracting prior to the application of the electric-field pulse. Once the tuning pulse is applied, neighboring atoms are coupled via V_{DD}, and population can be transferred from the initial pair state ψ_0 to ψ'. In the short-pulse regime, the relative motion of atoms in a pair is negligible during the tuning pulse duration, τ, and therefore V_{DD} is constant for each pair. Assuming the tuning pulse is applied at a time $t = 0$, the probability for finding the pair in state ψ' after the pulse is given by the standard two-level Rabi formula,

$$|C'(\mathcal{T})|^2 = \frac{V_{\mathrm{DD}}^2}{\Omega^2} \sin^2 \Omega\mathcal{T}, \quad (19)$$

where $\Omega = \sqrt{\frac{1}{4}E^2 + V_{\mathrm{DD}}^2}$ is the Rabi frequency and E is the energy splitting between the two uncoupled levels ψ_0 and ψ'. The resonance line shape for a given value of $\mathcal{T} = \tau$ is obtained by plotting the population transfer as a function of E.

In the long-pulse regime, neighboring atoms move past each other at a distance of closest approach (or impact parameter), b, in a time $\tau_c \sim 2b\Delta v$, which can be much less than τ. In this case, the interaction time for a given pair of atoms $\mathcal{T}$ is limited to a time comparable to the collision time for that pair, τ_c. Unfortunately, because V_{DD} varies with time, the detuning dependence of the transition probability, from ψ_0 to ψ', cannot be expressed in closed form. However, Eq. (19) can be used still to determine the approximate dependence of the resonance width on Δv. To do so, we assume a constant interaction $V_{\mathrm{DD}} = \mu_A\mu_B/b^3$ over a time $\mathcal{T} = \tau_c$. Note that the time integral of this approximate, constant potential is equal to that of the actual time-dependent potential [24,34].

The experiments are performed with ensembles of atoms with a distribution of different relative velocities and impact parameters. Therefore, in all of the measurements, $\mathcal{T}$ is determined primarily by τ_c for some atom pairs (long-pulse regime) and by τ for others (short-pulse regime). The demarcation between the long- and short-pulse regimes for the ensemble measurement is, therefore, only approximate, and requires that one identify the relative velocity and separation of atoms that are the majority contributors to the signal. Therefore, we define a critical impact parameter, b_0, as the largest value of b for which the on-resonance ($E = 0$) transition probability is a maximum ($|C'|^2 = 1$). In this case the argument of the sine in Eq. (19) is $\Omega\mathcal{T} = V_{\mathrm{DD}}\tau_c = \pi/2$, or

$$\frac{\mu_A\mu_B}{b_0^3}\frac{2b_0}{\Delta v} = \frac{\pi}{2}. \quad (20)$$

Solving for b_0, we obtain [24,34]

$$b_0 = 2\sqrt{\frac{\mu_A\mu_B}{\pi\Delta v}}. \quad (21)$$

Atom pairs with $b \leqslant b_0$ are the predominant contributors to the resonant energy transfer signal. If left on resonance, the typical interaction time for atom pairs with the critical impact parameter is $\tau_0 = 2b_0/v_0$, where $v_0 = \sqrt{\frac{2kT'}{\pi\kappa M}}$ is the average relative speed of Rydberg atoms in the ensemble. Accordingly, the duration of the tuning pulse relative to this critical interaction time determines whether a measurement is performed in the short-pulse regime ($\tau < \tau_0$) where the interaction is limited by the tuning pulse duration, or in the long-pulse regime ($\tau > \tau_0$) where the motion of neighboring atoms defines the interaction time.

For all of the measurements reported here, $\mathcal{T} \ll V_0^{-1}$. In effect, the resonances are Fourier-transform broadened by the limited interaction time and, when integrated over the ensemble, the contribution of the "natural" linewidth $4V_0$ to the resonance line shape is negligible. By ignoring V_{DD} compared to E in our constant potential approximation, the line shape given by Eq. (19) becomes

$$|C'(\mathcal{T})|^2 = V_{\rm DD}^2 \mathcal{T}^2 \,{\rm sinc}^2(E\mathcal{T}/2), \tag{22}$$

which has a FWHM energy width, $\Delta E \simeq \sqrt{32}/\mathcal{T}$ (a.u.). Thus, as the duration of the tuning pulse is decreased in the short-pulse regime, we expect the resonance linewidth to increase as $1/\tau$. Similarly, in the long-pulse regime, the linewidth scales as $1/\tau_0 = \frac{v_0}{2b_0}$. In this case, Eq. (21) can be used to obtain an approximate expression for the linewidth in terms of the average relative speed and relevant constants,

$$\Delta E \simeq \sqrt{\frac{2\pi}{\mu_A \mu_B}}\, v_0^{3/2}. \tag{23}$$

This approximation should predict accurately the velocity dependence of the resonance width, even though the functional form of the observed line shape is not actually a sinc^2. The correct line shape depends on the details of the time-dependent interaction potential for each atom pair, integrated over the relative velocity and position distribution functions for the ensemble [7,11,24,34].

It is worth noting that for long expansion times, $\sqrt{\kappa} \simeq \frac{\Delta t}{d}\sqrt{\frac{kT'}{M}}$, so $v_0 \simeq \sqrt{\frac{2}{\pi}}\frac{d}{\Delta t}$ depends only on the excitation laser diameter and the expansion time. In this case, provided $\tau_0 \ll V_0^{-1}$, the resonance width is independent of the initial beam density and temperature and can be expressed as

$$\Delta E \simeq \left(\frac{32}{\pi \mu_A^2 \mu_B^2}\right)^{1/4} \left(\frac{d}{\Delta t}\right)^{3/2}. \tag{24}$$

E. On-resonance population transfer

In the long-pulse regime, the magnitude of the population transfer at the peak of the resonance line shape is directly related to the Rydberg atom density at a given expansion time, Δt. The number of atom pairs undergoing population transfer is straightforward to calculate if one treats the energy exchange process as a collision [24]. In this case, if the atoms remain in resonance for a duration τ, then the number of atom pairs that are collisionally excited from ψ_0 to ψ' is

$$N' = N_0 \rho \sigma v_0 \tau \approx 4 N_0 \rho \mu_A \mu_B \tau, \tag{25}$$

where $\sigma = \pi b_0^2$ is the effective collision cross section, N_0 is the number of Rydberg atom pairs initially in ψ_0, and N' is the number of atom pairs in ψ' after a time τ. Thus, the on-resonance population transfer probability for a given expansion factor κ can be written as

$$P_0 = N'/N_0 \approx 4\rho_0 \mu_A \mu_B \tau/\sqrt{\kappa}. \tag{26}$$

Equations (25) and (26) are valid provided $N' \ll N_0$, as is the case for all of the measurements taken for $\Delta t \geqslant 500$ ns.

V. COMPARISON WITH EXPERIMENT

The expressions derived in Sec. IV can, in principle, be used to (i) determine the reduction in the effective temperature of the Rydberg sample for increasing pulse delays Δt, (ii) predict the decrease in the resonance linewidths ΔE and maximum population transfer P_0 with increasing Δt, and (iii) compute the increase in the resonance linewidths owing to coherent Fourier transform broadening as the tuning pulse duration, τ, is decreased at a fixed expansion time Δt. However, to do so requires knowledge of the K oven temperature, initial beam density, and the diameter of the cylinder of Rydberg atoms initially excited by the focused laser beams. These parameters could not be measured accurately in the experiment. However, we can extract their values by fitting the measured delay dependence of ΔE and P_0 in the long-pulse regime. The best-fit values allow us to predict the transform-limited widths of the resonances for the controlled interactions in the short-pulse regime. The calculated values are found to be in good agreement with our measurements.

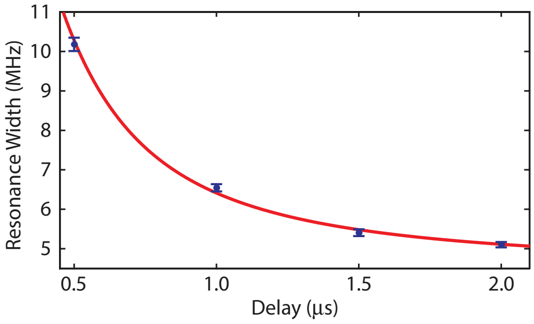

FIG. 4. (Color online) Resonance widths ΔE plotted as a function of expansion time Δt. The solid line is a least-squares fit to the data points assuming the resonance widths include homogeneous and inhomogeneous contributions, with the homogeneous width given by Eq. (24). The laser beam diameter, $d_0 = 127 \pm 2$ μm, and the inhomogeneous width, $\Delta E_i = 4.47 \pm 0.05$ MHz, are the fit parameters.

For long expansion times $\Delta t \geqslant 500$ ns, the resonance widths ΔE are essentially independent of the initial beam temperature [see Eq. (24)]. Therefore, the laser beam diameter, d_0, is used as a fit parameter within Eq. (24) to reproduce the linewidths of resonance curve data similar to that shown in Fig. 2. Figure 4 shows the best fit to the resonance width data, which is obtained for $d_0 = 127 \pm 2$ μm. This beam diameter is consistent with expectations based on the experimental focusing geometry. The fit includes an inhomogeneous broadening contribution, $\Delta E_i = 4.47 \pm 0.05$ MHz, added in semiquadrature to the homogeneous resonance width obtained from Eq. (24). This additional broadening can be attributed to the presence of electric-field inhomogeneities, on the order of 150 mV/cm, in the interaction region.

The inferred value for d_0 can be used to determine the initial K beam density and temperature by comparing the measured expansion time dependence of the on-resonance population transfer with that predicted by Eq. (26). For $\Delta t = 0$, the magnitude of the on-resonance signal saturates at the level shown in Fig. 2 for on-resonance times $\tau > 1$ μs. Therefore, that maximum signal level represents a population transfer probability, $P_0 = 1/2$, and can be used to normalize the resonance curves taken at different expansion times. In this way, the peak signal amplitudes can be directly compared to the population transfer probabilities from Eq. (26).

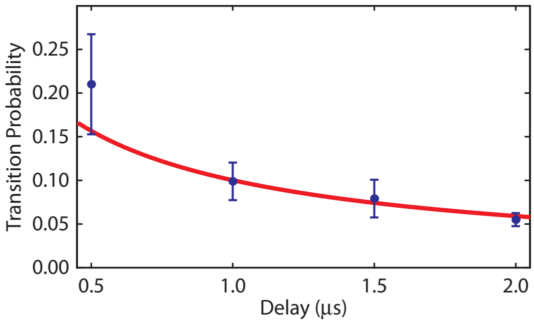

FIG. 5. (Color online) On-resonance transition probability, P_0, as a function of expansion time for a fixed tuning pulse duration, $\tau = 1$ μs. The data points are the measured transition probabilities. The solid line is the best fit of Eq. (26) to the data, obtained with $T = 523 \pm 3$ K.

The density of K atoms in our effusive beam at a distance L in front of the exit hole in the oven source is

$$\rho_K = 6.5 \times 10^{17} \frac{\mathcal{P} A_o}{L^2 T} \text{ cm}^{-3}, \tag{27}$$

where $\mathcal{P}$ is the K vapor pressure inside the oven in Torr, $A_o = 0.002$ cm^2 is the area of the exit hole in the thin walled oven, $L = 26$ cm is the distance from the oven to the laser excitation region, and T is the temperature of the oven and the K beam in degrees Kelvin [35,36]. Each of the three dye lasers saturates their respective transitions. Therefore, immediately following the laser excitation, the $4s$, $4p$, $29s$, and $27d$ levels are uniformly populated and the initial density in each of the two Rydberg states is $\rho_0 = \rho_K/4$. By using the known temperature dependence of the vapor pressure, $\mathcal{P}$, for potassium [37], Eq. (27) is used to express ρ_0 as a function of T,

$$\rho_0 = \exp(-1.73 \times 10^5/T^2 - 9.29 \times 10^3/T + 36.2), \tag{28}$$

for T in degrees Kelvin and ρ_0 in cm^{-3}. From this expression, Eq. (26) can be written in terms of T and known constants. As shown in Fig. 5, we use Eq. (26) with T as a fit parameter to reproduce the measured decrease in the on-resonance transition probability P_0 with increasing expansion time Δt. The best fit yields $T = 523 \pm 3$ K, which corresponds to an initial Rydberg density of $\rho_0 = 5.4 \times 10^7$ cm^{-3}.

Recall that in using Eq. (24) to determine the beam diameter d_0, we implicitly neglected the small temperature dependence of the resonance widths at long expansion times. If we use $T = 523$ K and Eq. (23) to refit the linewidth data as a consistency check, we find negligible differences in the two values for d_0.

Following the determination of the laser beam diameter, initial Rydberg density, and temperature, we can quantify the degree of effective cooling achieved in the experiment. Specifically, for $\Delta t = 2$ μs, $\kappa \simeq 63$, and the effective beam temperature is reduced from 523 to 8 K. At these low effective temperatures, the tuning pulse duration, and not the relative motion of atom pairs, determines the length of time that typical atoms interact. The reduction in interaction time with decreasing τ is reflected by an increase in the measured resonance widths. Figure 6 shows the measured and calculated variation in the resonance linewidth as a function of τ for a fixed expansion time, $\Delta t = 1.5$ μs. Here the critical interaction time defining the long- and short-pulse regimes is $\tau_0 = 490$ ns. The data for $\tau \geqslant \tau_0$ agree with the calculated width for RET in the long-pulse regime. Conversely, for $\tau \leqslant \tau_0$, the measured widths are in good agreement with the short-pulse prediction, $\Delta E = \sqrt{32}/\tau$. It is in this short-pulse regime that coherent interactions between all atoms begin and end at the same times. Accordingly, the coherence of the interaction can be exploited and controlled in a predictable way [9,27,31].

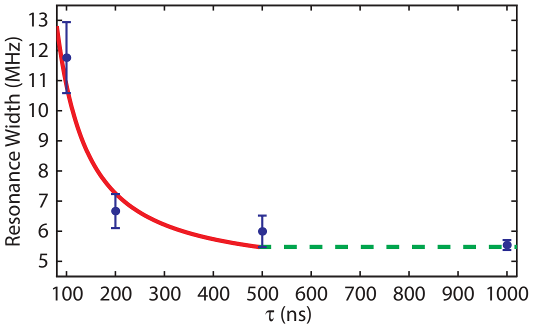

FIG. 6. (Color online) Resonance widths ΔE as a function of tuning pulse duration τ for a fixed expansion time, $\Delta t = 1.5$ μs. The data points are the widths of measured resonances, similar to those shown in Fig. 3. Under these conditions, $\tau_0 = 490$ ns separates the long- and short-pulse regimes. The dashed line denotes the predicted width in the long-pulse regime, where $\tau > 490$ ns [i.e., for Eq. (23) added in semiquadrature to the 4.5-MHz inhomogeneous width discussed in the text]. The solid line is the predicted width for the short-pulse regime, where $\tau < 490$ ns (i.e., for $\Delta E = \sqrt{32}/\tau$ added in semiquadrature to the inhomogeneous width).

VI. SUMMARY AND CONCLUSION

A laser-based atomic beam chopper has been used to reduce the relative velocities of Rydberg atoms in an effusive beam, enabling control over coherent RET between atoms. A reduction by more than a factor of 60 in the effective temperature of K atoms in an effusive beam is achieved. Significant Fourier-transform broadening of electric-field tuned resonances is observed as the allowed time of interaction between atoms is reduced below the time scale for collisions between typical atom pairs. This coherence can be exploited to enable pulsed-field control of DD interactions.

The laser-chopper technique demonstrated and analyzed here offers a straightforward approach for achieving transform-limited Rydberg-Rydberg interactions without the need for laser cooling and/or trapping. Indeed, if used in conjunction with a supersonic expansion, effective temperatures well below 1 K might be produced. For example, for a beam initially at 1 K, the effective temperature of the interacting atoms can be reduced to 10 mK by using an expansion time of $\Delta t \sim 10$ μs and a Rydberg excitation beam diameter of $d \sim 25$ μm. More generally, the method might be effective for studying interactions between cold atoms or molecules that have been laser excited to metastable, or stable, neutral, or ionic states.

ACKNOWLEDGMENTS

This work has been supported by the AFOSR and the NSF.

[1] D. Jaksch, J. I. Cirac, P. Zoller, S. L. Rolston, R. Cote, and M. D. Lukin, Phys. Rev. Lett. **85**, 2208 (2000).

[2] M. D. Lukin, M. Fleischhauer, R. Cote, L. M. Duan, D. Jaksch, J. I. Cirac, and P. Zoller, Phys. Rev. Lett. **87**, 037901 (2001).

[3] L. Isenhower, E. Urban, X. L. Zhang, A. T. Gill, T. Henage, T. A. Johnson, T. G. Walker, and M. Saffman, Phys. Rev. Lett. **104**, 010503 (2010).

[4] M. P. Robinson, B. Laburthe Tolra, M. W. Noel, T. F. Gallagher, and P. Pillet, Phys. Rev. Lett. **85**, 4466 (2000).

[5] F. Robicheaux and J. D. Hanson, Phys. Rev. Lett. **88**, 055002 (2002).

[6] W. Li, P. J. Tanner, and T. F. Gallagher, Phys. Rev. Lett. **94**, 173001 (2005).

[7] D. S. Thomson, R. C. Stoneman, and T. F. Gallagher, Phys. Rev. A **39**, 2914 (1989).

[8] D. S. Thomson, M. J. Renn, and T. F. Gallagher, Phys. Rev. Lett. **65**, 3273 (1990).

[9] M. J. Renn and T. F. Gallagher, Phys. Rev. Lett. **67**, 2287 (1991).

[10] M. J. Renn, W. R. Anderson, and T. F. Gallagher, Phys. Rev. A **49**, 908 (1994).

[11] J. R. Veale, W. Anderson, M. Gatzke, M. Renn, and T. F. Gallagher, Phys. Rev. A **54**, 1430 (1996).

[12] W. R. Anderson, J. R. Veale, and T. F. Gallagher, Phys. Rev. Lett. **80**, 249 (1998).

[13] I. Mourachko, D. Comparat, F. de Tomasi, A. Fioretti, P. Nosbaum, V. M. Akulin, and P. Pillet, Phys. Rev. Lett. **80**, 253 (1998).

[14] W. R. Anderson, M. P. Robinson, J. D. D. Martin, and T. F. Gallagher, Phys. Rev. A **65**, 063404 (2002).

[15] I. Mourachko, W. Li, and T. F. Gallagher, Phys. Rev. A **70**, 031401 (2004).

[16] T. J. Carroll, K. Claringbould, A. Goodsell, M. J. Lim, and M. W. Noel, Phys. Rev. Lett. **93**, 153001 (2004).

[17] S. Westermann, T. Amthor, A. L. de Oliveria, J. Deiglmayr, M. Reetz-Lamour, and M. Weidemuller, Eur. Phys. J. D **40**, 37 (2006).

[18] T. Vogt, M. Viteau, J. Zhao, A. Chotia, D. Comparat, and P. Pillet, Phys. Rev. Lett. **97**, 083003 (2006).

[19] B. Sun and F. Robicheaux, Phys. Rev. A **78**, 040701 (2008).

[20] T. Vogt, M. Viteau, A. Chotia, J. Zhao, D. Comparat, and P. Pillet, Phys. Rev. Lett. **99**, 073002 (2007).

[21] P. Bohlouli-Zanjani, J. A. Petrus, and J. D. D. Martin, Phys. Rev. Lett. **98**, 203005 (2007).

[22] C. S. E. van Ditzhuijzen, A. F. Koenderink, J. V. Hernández, F. Robicheaux, L. D. Noordam, and H. B. van Linden van den Heuvell, Phys. Rev. Lett. **100**, 243201 (2008).

[23] N. Saquet, A. Cournol, J. Beugnon, J. Robert, P. Pillet, and N. Vanhaecke, Phys. Rev. Lett. **104**, 133003 (2010).

[24] T. F. Gallagher, *Rydberg Atoms* (Cambridge University Press, New York, 1994).

[25] T. Forster, Ann. Phys. **437**, 55 (1948).

[26] R. C. Stoneman, M. D. Adams, and T. F. Gallagher, Phys. Rev. Lett. **58**, 1324 (1987).

[27] M. R. Kutteruf, Ph.D. thesis, University of Virginia, 2010.

[28] A. Reinhard, T. C. Liebisch, B. Knuffman, and G. Raithel, Phys. Rev. A **75**, 032712 (2007).

[29] A. Reinhard, K. C. Younge, T. C. Liebisch, B. Knuffman, P. R. Berman, and G. Raithel, Phys. Rev. Lett. **100**, 233201 (2008).

[30] R. Heidemann, U. Raitzsch, V. Bendkowsky, B. Butscher, R. Low, L. Santos, and T. Pfau, Phys. Rev. Lett. **99**, 163601 (2007).

[31] M. J. Renn, D. S. Thomson, and T. F. Gallagher, Phys. Rev. A **49**, 409 (1994).

[32] F. Reif, *Fundamentals of Statistical and Thermal Physics* (McGraw-Hill, New York, 1965).

[33] F. Robicheaux, J. V. Hernandez, T. Topcu, and L. D. Noordam, Phys. Rev. A **70**, 042703 (2004).

[34] D. S. Thomson, Ph.D. thesis, University of Virginia, 1990.

[35] *Experimental Methods in the Physical Sciences: Atomic, Molecular and Optical Physics: Atoms and Molecules*, edited by F. B. Dunning and R. G. Hulet (Academic Press, San Diego, 1996).

[36] *Atomic and Molecular Beam Methods*, edited by G. Scoles (Oxford University Press, New York, 1988), Vol. 1.

[37] B. Shirinzadeh and C. C. Wang, Appl. Opt. **22**, 3265 (1983).